The applicability and accuracy of computer modeling in regards to acoustical scattering by a complex geometry

by

William J. Elliot

Submitted to the Department of Architecture
in partial fulfillment of the
Requirements of the Degree of

Bachelor of Science

at the

Massachusetts Institute of Technology

June 2005

Signature of Author _____
Department of Architecture
May 13, 2005

Certified by _____
Carl Rosenberg
Department of Architecture, Lecturer in Acoustics
Thesis Supervisor

Accepted by _____
Adèle Naudé Santos
Acting Head, Department of Architecture
Dean, School of Architecture and Planning

The applicability and accuracy of computer modeling in regards to acoustical scattering by a complex geometry

by

William J. Elliot

Submitted to the Department of Architecture
On May 13, 2005 in partial fulfillment of the
Requirements for the Degree of Bachelor of Science in
Art and Design

Abstract

The intent of the investigation is to try to characterize the nature of scattered acoustical energy off of the face of a concrete masonry unit with an atypical geometry. The nature of the tests conducted would be in accordance with the AES-4id-2001 document which pertains to the *Characterization and measurement of surface scattering uniformity*. The uniformity of scattering can be analyzed and can give one an indication of the diffusive properties of the test samples.

The product for which the testing is proposed, as previously mentioned, is a modification of a concrete masonry unit. The product is *not* uniform in section, a fact which means a two dimensional analysis of scattering will not suffice. Instead, the distribution of reflected sound waves over a hemispherical shell will be examined.

Thesis Supervisor: Carl Rosenberg
Title: Department of Architecture Lecturer in Acoustics

Contents

Introduction

Beginning with the pioneering work completed by Wallace C. Sabine in the early 1900's, acousticians have become increasingly knowledgeable of the mechanisms which govern sound absorption. The dissipation of sound energy as heat due to viscous boundary layer effects is the prime method by which sound is attenuated (Cox and D'Antonio, 129). This dissipation is then related to the porosity and the flow resistivity of the material in question.

Any building material employed in construction will undoubtedly be exposed to a plethora of frequencies. Such frequencies may indeed be subsonic or super sonic. Of course, the frequencies of most interest for acoustical phenomena are naturally those which are within the audible frequency range. The audible frequency range for humans is 20 Hz to 20,000 Hz.

Indeed, the interior space of a concert hall will encounter many more sounds than a pure tone propagated at a single frequency. With the change in frequency comes a change in wavelength, dictated by the well known relation:

$$\lambda = {}^{c}/_{\nu} \qquad (1)$$

As the wavelength changes, so to does the interaction of the sound wave with the absorptive material. This is due to the difference in scale between the wavelength and the structure of the absorber itself. It follows that for a porous, homogenous material, the amount of absorption is a function of the wavelength (or frequency) of the incident sound wave. It is also possible to engineer resonant absorbers, however, such a discussion is beyond the scope of this paper.

One can certainly plot the relationship between sound frequency and the absorption by a specific material, but it is often convenient to divide the range of audible frequencies up into "benchmarks" so that one may more easily grasp the performance of the absorber. These "benchmarks" are known as frequency bands, or octave bands.

An octave is defined as the range of frequencies between an initial frequency and twice that frequency (in the Western musical tradition, a musical scale contains eight notes that span this range, hence the name, *octave*). An octave band is denoted by the frequency at its geometric center. For example, the 125 Hz octave band covers a range of frequencies from approximately 89 Hz to 178 Hz.

For the purpose of testing absorption and transmission loss in a laboratory setting, the frequencies between 100 Hz and 4000 Hz are examined (Cavanaugh, 6-7). For the purpose of this investigation the 500 Hz, 1000 Hz, 2000 Hz, and 4000 Hz frequency bands will be examined (this condition applies to the testing within the CATT-Acoustic Software, where results are given in frequency bands).

Absorption is only one acoustical criterion that affects the architectural space with which it interacts. The reflective properties of a material are also important. Surface irregularities as well as how the surface is articulated by the architect/engineer affect how sound interacts with said surfaces, and therefore how the reflected sound is distributed throughout the environment. This is the crux of the current thesis investigation.

Several absorption tests have been standardized, but the subject of a standardized test for scattering or diffusion is still under debate. In an effort to make this investigation as lucid as possible, both of these terms are defined below. While diffusion is clearly a corollary to scattering, it is the scattering properties of a sample which will be examined in this thesis.

> *scattering* - refers to the sound energy that is distributed in a non-specular manner as plotted in a polar response. Scattering is frequency dependent, and it is dependent on the angle of incidence
>
> *diffusion* – a measure of the uniformity of the reflected sound (Cox and D'Antonio, 87)

One will note that the definition of scattering includes the term *non-specular*. This refers to how the sound waves are reflected from a surface. For the sake of simplicity, imagine a sound wave as a series of parallel rays striking a surface. In a specular reflection the rays reflected from the surface maintain an ordered orientation (a beam of incoming sound "rays" will be reflected as a beam of sound rays). In the non-specular case, the reflected rays have a very disordered orientation, and no one reflected beam is evident. Figure 1 illustrates the difference between specular and non-specular reflections (Hecht, 99).

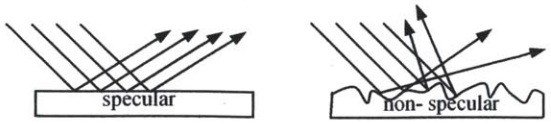

Figure 1

In each case the rays are reflected at an angle equal to the angle of incidence, however, surface irregularities give rise to the non-specular case. For this thesis, the term scattering is used to refer to the distribution of sound energy reflected from the surface of a test sample. For this investigation, the test sample has a geometry which is irregular when compared to the control, and therefore "scattering" may loosely be used to describe the behavior of the reflected sound.

The sample product examined in this thesis is a modification of a concrete masonry unit (CMU). Two computer programs will be utilized to examine the nature of acoustical scattering by the CMU over the frequency ranges described in the introduction. The same setup will be utilized within each modeling program; the setup corresponds to one proposed laboratory configuration for evaluating acoustical scattering. The first computer program, CATT-Acoustic, is used primarily to examine room acoustics. CATT software (***C**omputer **A**ided **T**heater **T**echnique*) was originally developed as a theater lighting software, but the principals of ray tracing can easily be applied to acoustics (i.e. the field of geometric acoustics). The second computer program, ANSYS, has been used extensively in fluid, electromagnetic, and structural analysis. This software package is also capable of pressure wave analysis, and it is therefore applicable to this thesis investigation. ANSYS utilizes Finite Element Analysis to predict fluid-solid interactions; it has the potential to confirm or refute the findings of the CATT-Software using a different method to the same end, namely, analyzing the scattering by the CMU.

Geometry and Physical Characteristics of Test Sample

Careful measurements were taken from a sample block provided by the Proudfoot Company, which manufactures the *Sound Cell* ® block (i.e. the sample being investigated). Using these measurements, a three-dimensional computer model was constructed using AutoCAD. It is this model that could be imported into CATT-Acoustic or ANSYS for further analysis.

The figures on the following pages illustrate the size and physical configuration of the block. One important aspect to note about the geometry of the block is that it is *not* uniform in section. A sample uniform in section could easily be analyzed for scattering with a two dimensional testing configuration (the scattering would be invariant to a change in the z-coordinate of the source, so long as the source aim remained normal to the block face). Because the section of the block changes with changes in the z-coordinate, scattering must be examined with a three dimensional testing configuration. The specific form of the laboratory setup will be explained in detail in a subsequent section of this paper.

The necessity for a three dimensional analysis of scattering from a sample may be more easily understood by examining the following figure. Figure 2 shows two blocks, one uniform in section (a simple extrusion of a square) and the other block varies in section with height. The dots represent different possible source positions, with the lines representing the path of sound from the corresponding source. The black arrows indicate the vector normal to the surface on which the sound is incident.

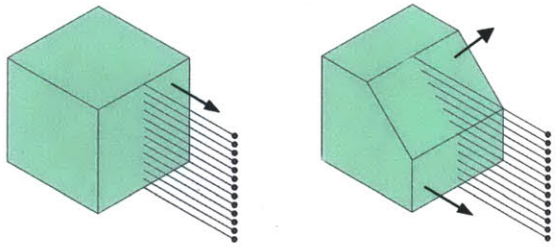

Figure 2

It is clear from the diagram that as one chooses different z-coordinates for the sound source, the scattering pattern will remain the same (there is no reason that a reflected ray has a z component other than 0) for the block that is uniform in section. In the case of second block, the splayed face has a normal vector which is not coincident with the incoming sound waves. In other words, over the splayed surface the incident angle of the incoming sound has changed, and therefore the nature of the reflected sound will change as well. In order to evaluate the behavior of the entire second block, one must look at how the reflected sound is distributed over *x*, *y*, and *z* coordinates.

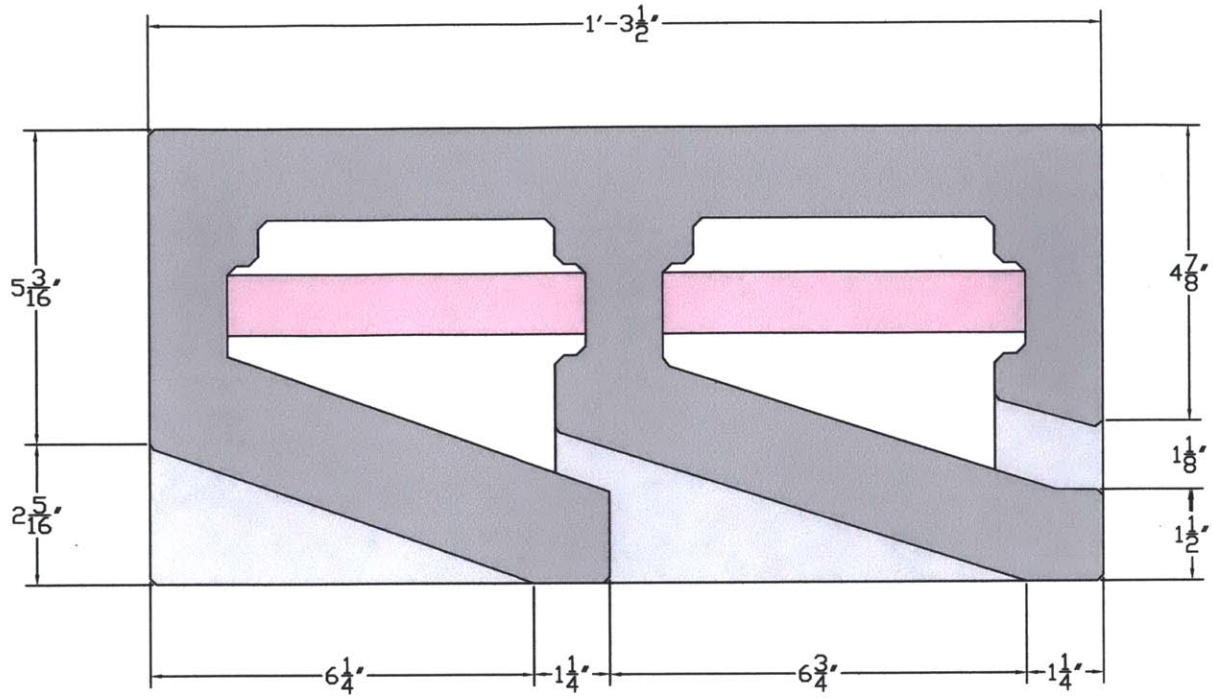

Figure 3a

Figure 3b

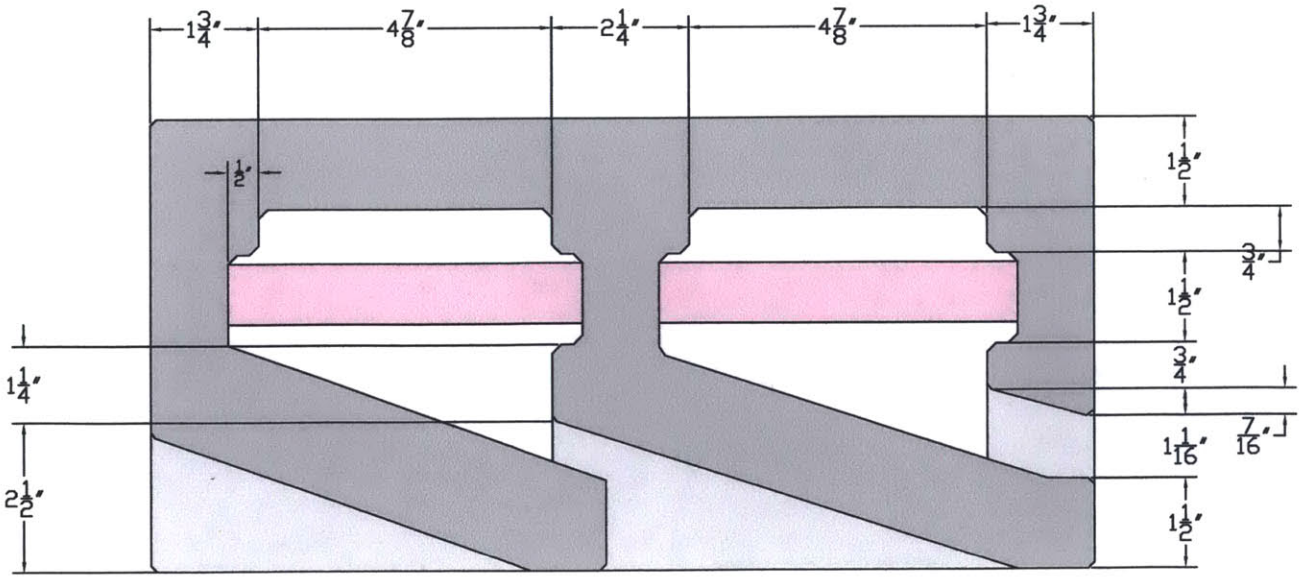

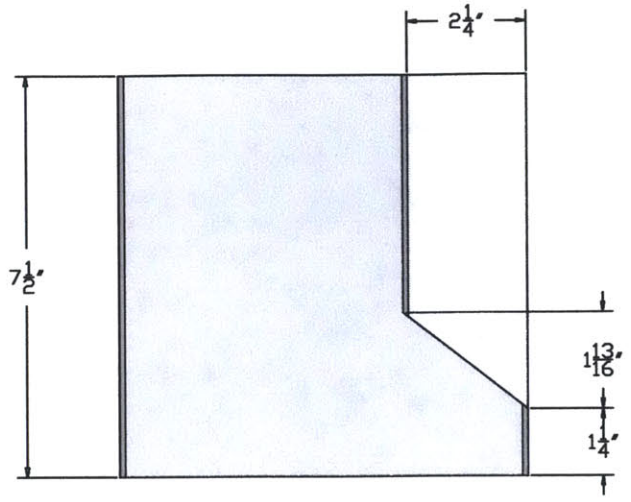

Figure 3c - left face

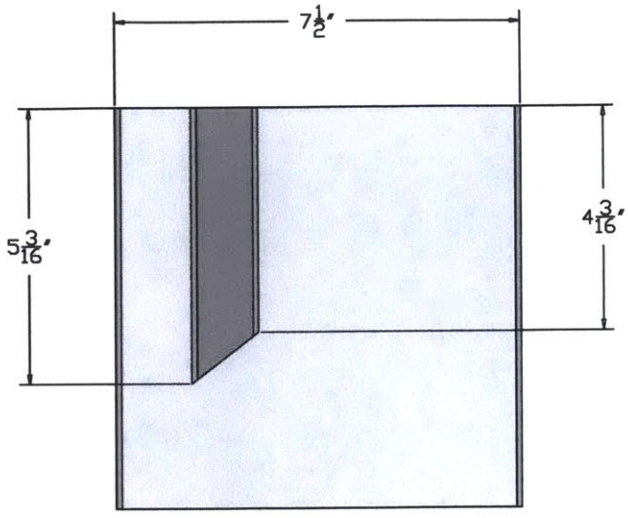

Figure 3d - right face

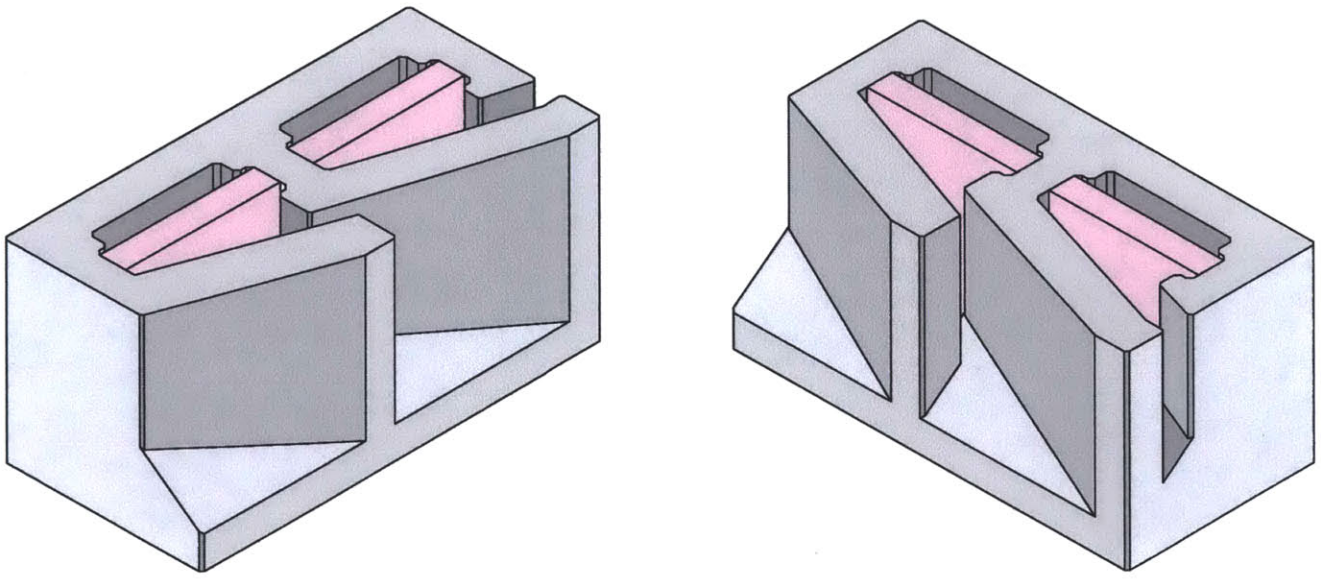

Figure 4 - isometric views

It should be noted that when the cavity within the block is closed off at the top and the bottom, a Helmholtz resonator is created. A Helmholtz resonator is created when a narrow opening gives way to a larger enclosed volume. A commonplace Helmholtz resonator is an empty glass bottle over which one blows air. The sound produced is the resonant frequency of the Helmholtz resonator. The resonant frequency of a Helmholtz resonator is given by the following equation (Morse, 490).

$$\omega_r = \omega_0/2\pi \qquad (2)$$

where ω_0 is defined as

$$\omega_0 = 2c\sqrt{\frac{S_0}{D_0 V_0}} \qquad (3)$$

V_0	*enclosed volume*
S_0	*area of constricted opening*
D_0	*perimeter of constriction*
c	*speed of sound*

Upon examining the block, ones see that each cavity within the block is filled with a piece of glass fiber insulation. This glass fiber effectively increases absorption over a broader range of frequencies.
The acoustical phenomenon presently described obviously applies to the process of absorption, not of scattering. It is important, however, to understand the motivation which resulted in the final form of the block.

It is obvious that the macroscopic form of the block will have an effect on the how sound waves interact at the block's surface. One may wonder, however, to what degree do small surface irregularities affect scattering by the block face. A close examination of the surface of a CMU reveals slight irregularities in the surface (e.g. compare with another surface such as polished marble). Figure 5 is a photograph of the surface of a standard CMU.

Figure 5

One can examine the degree to which such small surface irregularities contribute to the angle distribution of the scattered wave.

Let there be a surface in the *xy* plane, with a circular area *A* included on this plane. This circular area has a radius, *a* (see Figure 6). Within area *A*, the z coordinate of the surface is defined as follows $z = \eta(x, y)$. Over the rest of the surface, $z = 0$. The surface admittance within *A* can also be allowed to vary, but in this case the admittance is the same as that of the rest of the surface, β_0.

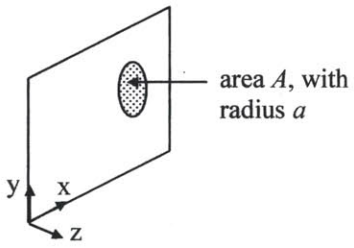

Figure 6

A detailed discussion of the derivation for the scattered angle distribution is given in *Appendix 1* on page 18. The equation for the scattered angle distribution is reproduced below for convenience.

$$\Phi(\theta_i, \varphi_i \mid \theta, \varphi) = \frac{ikwkh\cos\theta_i\cos\theta}{\pi(\cos\theta_i + \beta_0)(\cos\theta + \beta_0)}\left[\gamma^2 \frac{\sin(\mu_x \tfrac{1}{2})}{(\mu_x \tfrac{1}{2})}\frac{\sin(\mu_y \tfrac{1}{2})}{(\mu_y \tfrac{1}{2})}\right]$$

Figure 7 from *Appendix 1* has been reproduced below for the convenience of referring to angles which are included in equation (15).

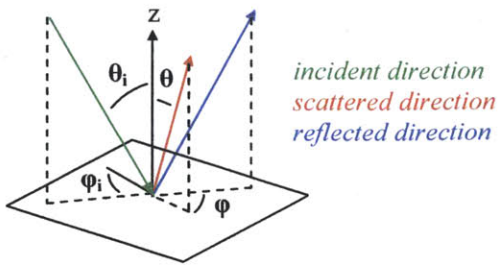

One has now arrived at an equation that describes the angle distribution of a scattered sound wave due to an irregularity in a planar surface. How does equation (15) apply specifically to the scattering induced by the Sound Cell block under investigation? As mentioned in the introduction, the frequencies utilized in testing this block are 500 Hz, 1000 Hz, 2000 Hz, and 4000 Hz. The corresponding wavelengths, measured in meters are 0.71, 0.35, 0.18, 0.09, respectively. As seen in Figure 5, the irregularities on the surface of the CMU are very small by comparison; indeed, the larger irregularities have a diameter of approximately 2.5 mm, or 0.0025 meters. Thus there is a one order of magnitude difference between the diameter and the shortest wavelength used in testing. In any case, for all of the frequencies used in testing, the corresponding wavelengths are all greater than the scale of the irregularity. This confirms that it was a correct assumption to use the Born approximation in deriving equation (15).

What exactly does equation (15) mean then in terms of testing procedures and the measured results? As given in equation (9), the scattered pressure is a function of Φ. Substituting various values for the incident and scattered angles into equation (15) for an irregularity on the order of 2.5 mm, one finds that Φ itself is very small. This is an important result; one need not concern oneself with disseminating between macroscopic scattering by the block shape and the "microscopic" scattering caused by surface irregularities since the irregularities do not give rise to a substantial scattered pressure wave in their own right.

Nature of Testing Setup

The physical orientation of the Sound Cell block in relationship to the sound source and receivers coincides with the guidelines stipulated in the Audio Engineering Society 4id-2001 document. This document, entitled *AES information document for room acoustics and sound reinforcement systems – Characterization and measurement of surface scattering uniformity*, suggests a possible standard procedure by which scattering may be measured. It is this procedure that was adapted to this thesis investigation and utilized in the acoustical modeling software.

One need not necessarily test the scattering properties of a sample in a completely open environment (i.e. no walls, ceiling, or floor that might affect sound propagation and scattering). Instead, there exist minimum room dimensions that approximate a "free field" where the contributions of reflections from the room boundaries are negligible.

While the AES 4id-2001 document describes in detail a two-dimensional setup for testing a diffuser that is uniform in section, the physical setup remains similar for the Sound Cell block, save for the arrangement of the acoustical receivers.

The two-dimensional setup is shown below in Figure 8

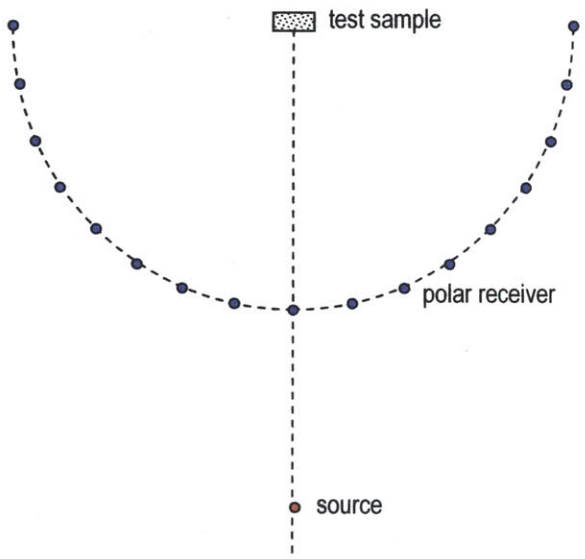

Figure 8

As can be seen in Figure 8, the polar array of receivers will monitor the sound reflected from the surface of the block, and by their very location indicate the angular dependence of scattered sound intensity.

This two dimensional layout can be used to specify the size of room in which the test for scattering will be performed. The testing configuration in Figure 8 is reproduced in Figure 9. *H* and *W* denote the axes of an ellipse. Point *s* represents the source location, point *r* represents the receiver location, and point *b* is coincident with the wall forming the boundary of the room.

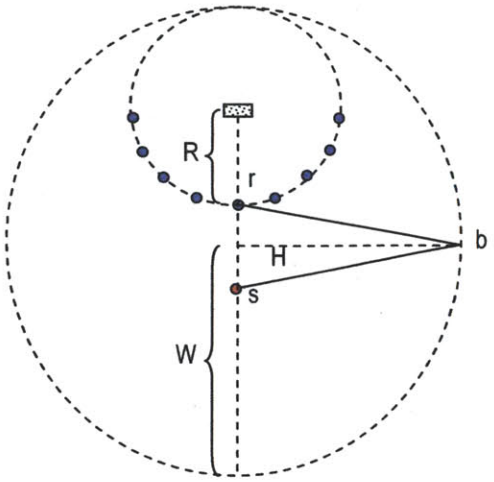

Figure 9

By inspection one can calculate the length of the *W*. Given that the ellipse is tangent to the circle of radius *R* which surrounds the sample and that *H* bisects a segment of length *R* which connects points *r* and *s*, one finds the length of *W* to be 2.5R. The length of *H* comes from the length of a second order reflection from the speaker (this involves a distance of 5R; the sound travels from *s* to the sample then back to *s* where the sound reflects off of the source and is recorded at the receiver). If this value of 5R is the limiting distance, then the path of sound from *s* to *b* and then to *r* must also equal 5R. Given that the base of the resulting isosceles triangle has a length of R, one can calculate the length of *H* to be approximately 2.45R.

One may then wonder what criteria are involved in specifying the distance R. According to the AES-4id-2001, suitable distances are defined in terms of a distance ř and its relationship to D_{max}, the largest dimension of the scattering surface. The distance ř is defined as follows:

$$\check{r} = \frac{2r_1r_2}{r_1+r_2} \qquad (17)$$

where r_1 = the distance from the source to a chosen reference point
r_2 = to distance from the receiver to the same chosen reference point

Measurements using the polar array of receivers would be done in the "far field," a configuration in which the following relationships apply (λ is the wavelength used in testing):

$\check{r} >> D_{max}$
$\check{r} / D_{max} >> D_{max} / \lambda$

Implementation of CATT-Acoustic Model

A solid model of the Sound Cell block was created from physical measurements (Figures 3a-3d). After placing 3D planes on each surface of the solid model in AutoCAD, the planes were exported to the CATT Acoustic Software (it is planar surfaces, not solid objects that are exchangeable between AutoCAD and CATT-Acoustic).

When defining 3D planes in AutoCAD, one is only able to specify four points (any 3D plane is restricted to being a quadrilateral). This is not the case with plane definition in CATT, however, and after importing a model one can combine smaller planes into larger surfaces to simplify the geometry of the model, and thereby reduce the calculation time. One must be confident, however, that every smaller plane is composed of points which are indeed coplanar.

The order in which one defines points on a 3D plane within AutoCAD also specifies the direction of the normal to that plane (in agreement with a right-handed coordinate system). While one could certainly make a conscious effort to always specify planes with a counter-clockwise series of points (outward facing normal), the orientation of the plane can easily be changed within CATT-Acoustic.

Initially it was decided to construct a hemispherical array of "receivers" in front of the Sound Cell block. These receivers function in CATT-Acoustic as spatial measurement points, and one can analyze certain acoustical parameters at each of these points. This hemisphere contains receivers spaced every 5° about the block (spanning from 0° to 180°) and every 5° of ascension from 0° to 85° measured with 0° at the floor of the testing room.

For each individual receiver, the level of sound attenuation produced by its distance from the sound source was calculated. It was intended that examining the difference between the predicted pressure level of the direct sound and the pressure level measured at each

receiver by CATT would help to characterize the amount of sound reflection that was influencing each receiver.

The amount of attenuation by distance is described by the following equation.

$$SPL_{receiver} = SPL_{source} - 20\log\left(d_2/d_1\right) \qquad (18)$$

In this case *SPL* stands for sound pressure level, as measured in decibels. The SPL at the source was defined over each frequency band as 90 dB measured at a distance of 1 meter (1 m = d_1). Thus, one need only calculate the second distance (from the source to d_2) to arrive at the SPL for each receiver. The distances from the source to each receiver, and the corresponding SPL levels of direct sound, are given in *Appendix 2* on page 20.

After running CATT models containing one Sound Cell Block, a 3x3 array of Sound Cell Blocks, and a 5x5 array of Sound Cell Blocks, the difference in SPL levels between the direct sound and that measured by CATT-Acoustic at each receiver was examined. The results from the 3x3 array of Sound Cell Blocks are reproduced in *Appendix 3* on page 22. For purposes of length, only the results from the 0° ascension polar array are given in the appendix.

In these preliminary tests, only the receivers at 0°, 15°, 30°, 45°, 60°, and 75° ascension were tested. It was intended that these increments would provide an adequate sampling of the acoustical behavior at receiver locations. If significant results were gained from these tests, it was then intended that each 5° increment of ascension would be tested and examined.

As one can see from the data in *Appendix 3*, the difference in SPL levels, presumably a result of the sound being scattered from the surface of the block, is very small indeed. In general, the minimum difference which can be perceived by the human ear (known as the *just noticeable difference*) is approximately 3 dB. An unfortunate drawback of examining each SPL receiver level is that within the CATT Program one cannot choose the time at which to measure the SPL for a given receiver. If this were possible, one could examine the time window in which the reflected rays were reaching the receivers. The SPL levels for each receiver instead reflect the sum of rays that reach the receiver over the time in which the rays are being traced.

Modification of CATT-Acoustic Model

Although the results from examining individual receivers placed on a hemisphere surrounding the Sound Cell block did not yield definitive results regarding scattering by the block, another method for testing the block could be utilized within the CATT-Acoustic Program.

Instead of utilizing individual receiver locations to determine scattering, one can create continuous surface component planes through which the reflected rays from the Sound Cell block pass. Such a setup is possible in CATT-Acoustic if one uses the option of *Audience Plane Mapping*. Two advantages of audience plane mapping over analyzing individual receivers are 1) one can specify the time window in which to observe the sound levels on a given plane and 2) one need not run multiple tests for different angles of ascension since the planes create the entire hemisphere on which scattered rays are incident.

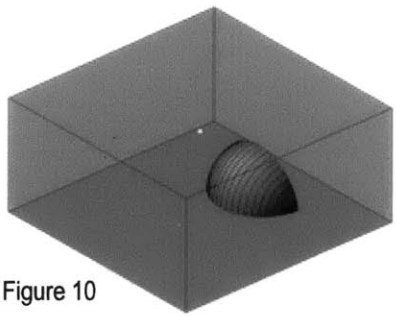

Figure 10

A view of the CATT-Acoustic model, including audience planes, is shown in Figure 10.

The planes in Figure 10 are not the actual audience planes, but rather they are present within the model because CATT-Acoustic requires reference planes from which to plot the audience plane maps, which contain acoustical data.

For any plane present in the CATT-Acoustic Model one needs to specify the material properties. For the purpose of this thesis investigation the following absorption coefficients were used for each element shown in Figure 10. Although one cannot see the Sound Cell block in Figure 10, it is present and is located at the center of the

sphere of which the hemisphere is a part. Table 1 gives the absorption coefficients for each aspect of the computer model, as well as the transparency coefficients for the hemisphere.

	Octave Band Frequency					
	125	*250*	*500*	*1000*	*2000*	*4000*
Walls	.99	.99	.99	.99	.99	.99
Concrete	.10	.05	.06	.07	.09	.08
Glass Fiber	.06	.20	.65	.90	.95	.98
Hemisphere	.01	.01	.01	.01	.01	.01
Hemisphere (transparency)	.99	.99	.99	.99	.99	.99

Table 1

As one is not permitted to have values such as 100% absorption or 100% transparency in CATT-Acoustic, values of 1% absorption and 99% transmission/transparency were assigned to the hemisphere. It should be noted that the hemisphere in Figure 10 is actually two hemispheres that are coincident, i.e. one needs to specify the properties on each side of the hemisphere. This is accomplished by making each plane that composes the hemisphere double-sided. The drawback of this requirement is that it doubles the number of planes composing the hemisphere and increases the time necessary for calculations. After constructing the model shown in Figure 10, some modifications had to be made. For example, CATT-Acoustic does not perform audience area mapping for planes whose normal vectors have a negative *z* component. This problem could easily be remedied by simply turning the model upside down. Thus, the final physical setup that was used is identical to that shown in Figure 11.

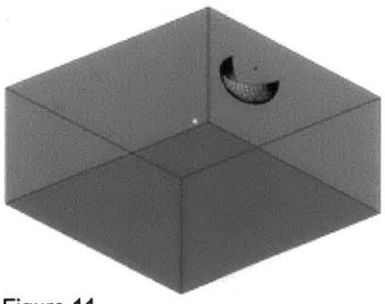

Figure 11

Initial Test Results

A series of tests were run in CATT-Acoustic using SPL mapping on audience planes that corresponded to the planes composing the hemisphere. Frequencies of 500 Hz, 1000 Hz, 2000 Hz, and 4000 Hz were examined for the following configurations:

- Empty room
- Single Sound Cell Block
- Single Flat CMU
- 3x3 Sound Cell Block array
- 3x3 Flat CMU array
- 5x5 Sound Cell Block array
- 5x5 Flat CMU array

The time intervals over which the audience planes were examined were chosen so as to coincide with the predicted arrival of reflected sound waves. The predicted arrival of the waves occurred after a period of 66.55 milliseconds. The time intervals chosen for audience mapping in each model are as follows: 55-60 msec, 60-65 msec, 65-70 msec, and 70-75 msec.

It seemed that initially the results of this approach for examining scattered sound rays were promising. The model of the empty room, however, revealed that the model was not behaving as it should. Since the hemisphere itself is transparent to sound, and the walls are 99% absorptive, the absence of a test sample should guarantee that no sound is reflected back onto the hemisphere. One should therefore have very low SPL levels plotted onto the audience planes above the hemisphere. This was not the result, however of the empty room model. Figure 12 shows that within each time interval, considerable SPL levels were recorded on the audience planes. The SPL scale is the same for each figure.

Obviously, modifications to the model were necessary if the control model (i.e. the empty room) was producing results that were not correct. It was suggested that the volume of the testing room be increased. Increasing the volume of the room would obviously move the walls further from the hemisphere and the testing sample location (at the center of the hemisphere). As seen in Figure 9, the minimum room size according to the *AES 4id-2001* document creates a situation in which the wall behind the sample location is coincident with the two-dimensional receiver array. In the case of a hemispherical array, the rear wall would be a plane tangent to the sphere of which the hemisphere is a part.

Figure 12

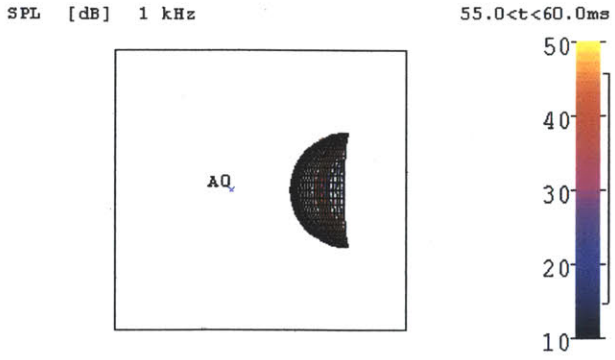

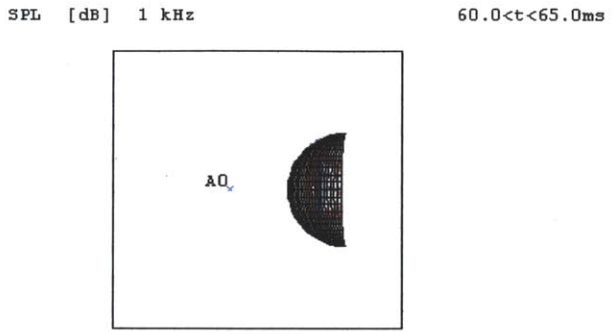

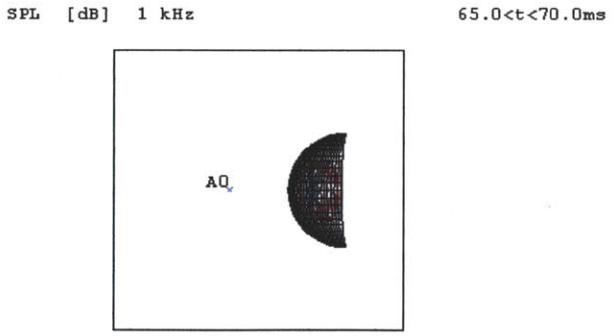

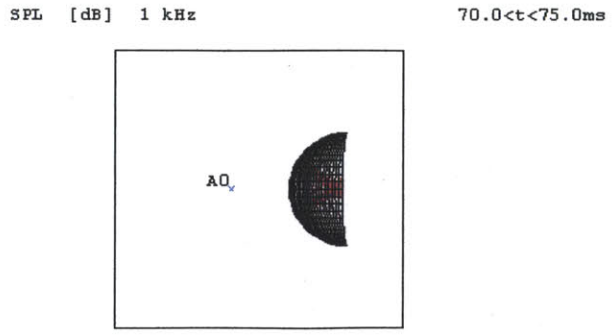

Each spatial coordinate defining a corner of an exterior wall was multiplied by a factor of 1.5 (one should note that the origin of the coordinate system within the CATT-Acoustic model was not at the corner of the room but rather near the center of the hemisphere, a default from importing the model from AutoCAD). The model increased in volume with this change from 26,563 m^3 to 89,646 m^3 (938,063.49 ft^3 to 3,165,818.61 ft^3). New models were run (see the list of configurations on the previous page) with this new volume. The results (shown for an empty room with a test frequency of 1000 Hz, compare with Figure 12) are displayed in Figure 13.

Figure 13

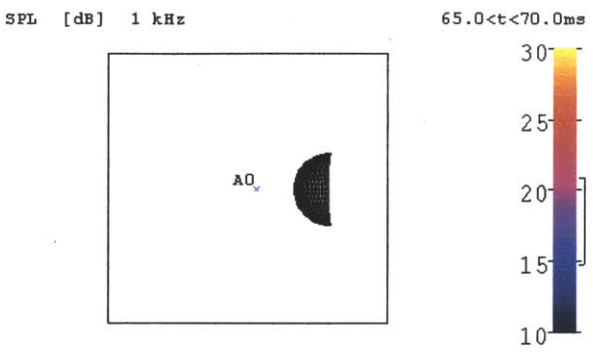

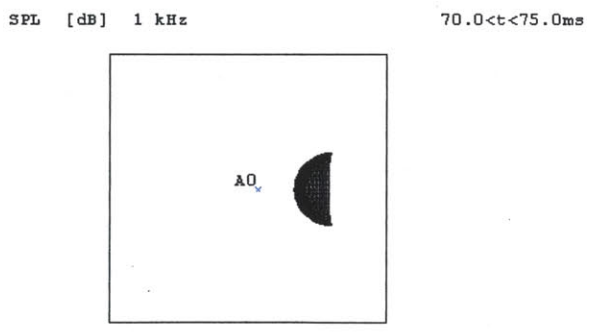

Data was not obtainable for the time intervals 55-60 msec and 60-65 msec; CATT-Acoustic simply did not produce audience mapping plots for these intervals, presumably because the SPL levels were negligible.

Thus, on first analysis one would presume that the problem involving the presence of SPL levels (when the test sample was absent) had been solved; the empty room model now indicated that very low SPL levels in the absence of a test sample. One could stipulate that the sound emitted at the source location was simply moving through the walls enclosing the testing setup, with minimal interaction (as evidenced by the very low SPL levels shown in Figure 13). Future tests could be compared involving sample blocks (Sound Cell and flat

CMU's) with the empty room model knowing that the acoustical interaction with the exterior walls was not having a great influence on the reported SPL levels on the audience planes.

After running the models using a room of increased volume, the audience plane plots were analyzed. The results for a 5x5 array of Sound Cell blocks with a test frequency of 1000 Hz are shown in Figure 14.

Figure 14

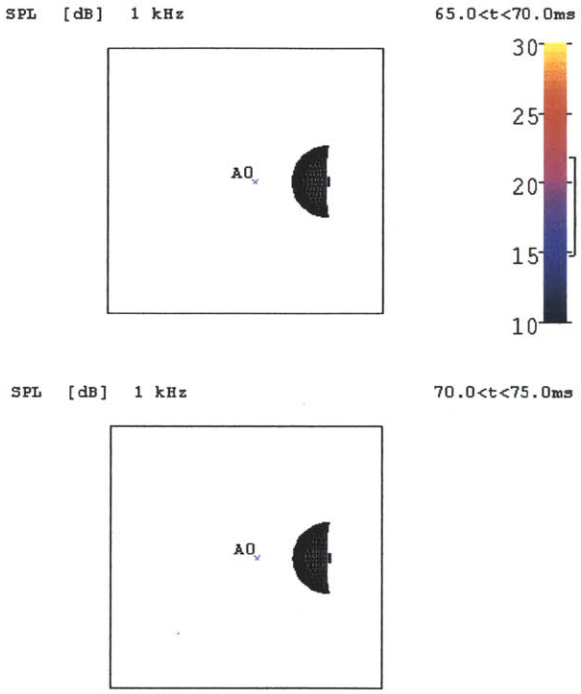

As with the empty room scenario, the first two time intervals were not plotted at all, and the two that were did not show any significant SPL levels on the audience planes. This was the case for all of the models which were run using the CATT-Acoustic software. Neither Sound Block arrays nor arrays of flat CMU's produced and significant SPL levels in the time intervals selected.

One more modification was made to the CATT-Acoustic models before the analysis using this software was deemed inconclusive. This modification is described in the next section.

Final Modification of CATT-Acoustic Model

All of the tests described in previous sections were carried out using a sound source that was omni-directional. In other words, the sound energy emanating from the source had no angular dependence and propagated equally in every direction.

It is possible within the CATT-Acoustic program, however, to modify the directionality of a sound source. This can be done to more accurately predict how certain types of sounds will be perceived within a space. For example, a trumpet certainly is a directional source; standing in front of the horn is much different than standing to the rear of the performer.

With the ability to create a very directional source, one was indeed created and aimed at the test sample within the CATT model. Figure 15 shows the distribution of sound energy for an omni-directional source and for the directional source that was created. These graphics are termed "polar balloons." The polar balloons show the sound energy for a certain spatial position. One can think of the polar balloon as a series of concentric spheres, with each surface corresponding to a decibel level (the dB levels decrease as one approaches the center of the spheres).

Figure 15

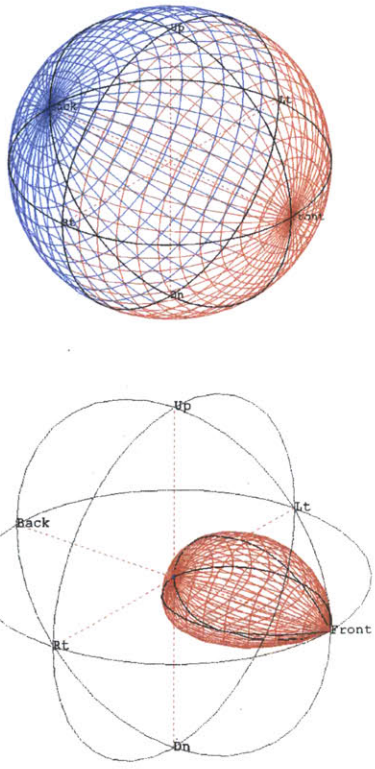

Results of Final Modification to CATT-Acoustic Model

The results for a 5x5 array of Sound Cell blocks with a test frequency of 1000 Hz are shown in Figure 16.

Once again, the data for the time intervals 55-60 msec and 60-65 msec were not reported. As can be seen in Figure 16, very low SPL levels were plotted on the audience planes. The results for different sized arrays of both flat CMU's and the Sound Cell blocks are consistent with the results shown in Figure 16.

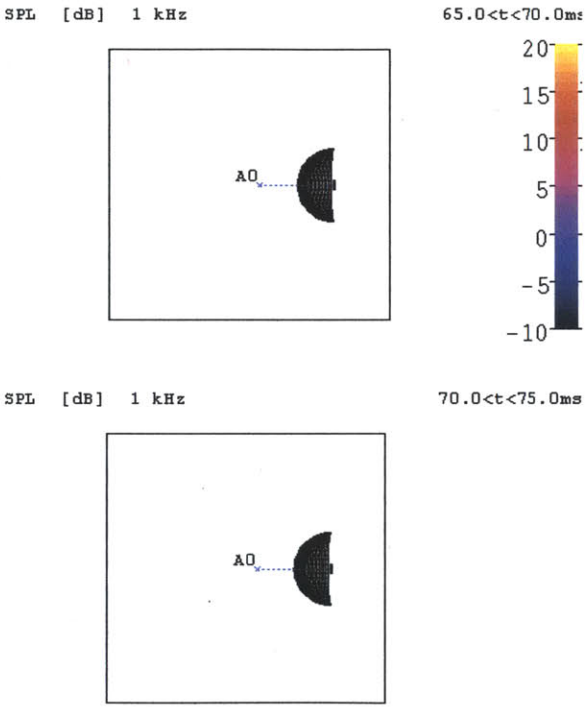

Figure 16

Evaluation of CATT-Acoustic as a predictive tool for scattering

Based on the results from several iterations of CATT-Acoustics models, it has been shown that given the nature of the input geometry, one cannot predict the scattering off of a surface.

Several limitations that are inherent in the CATT program may have contributed to the inconclusive results.

1) There is a limit to the number of planes which can be modeled within the program. Creating an array of planes for the audience area mapping and constructing an array of Sound Cell blocks quickly exceeds the number of allowable planes. It *is* possible that a larger array of blocks might yield some results, but in this case, the largest array that could be created without exceeding the 5000-plane limit was a 5x5 array of Sound Cell blocks.
2) CATT-Acoustic was designed primarily to predict acoustic parameters of *interior* spaces. Also, the larger the interior space created, the more the model resembles a free field (similar to being outdoors in a field, there are no nearby surfaces to introduce reflections). In the case of this investigation, a large room with 99% absorptive walls was created. Thus the model was both large, and "open" (99% of rays hitting the walls of the room were absorbed).
3) Within CATT-Acoustic one cannot choose the time interval to examine the SPL level of a receiver. Instead, the SPL levels at each receiver are recorded over the time interval in which the initial sound from the source is decaying. To avoid this limitation, audience plans were created for specific time intervals when reflections were predicted to be interacting with the hemispherical array of planes. This method has a drawback as well, however, in that the SPL levels for a given audience plane are a sum of incident sound over that interval. Thus, the shorter the interval, the fewer the number of rays that are summed to give an SPL level.

Another Approach to Scattering: Finite Element Analysis

As mentioned at the beginning of this paper, the second approach to evaluate scattering involved the use of Finite Element Analysis. Several software programs have been designed that perform FEA, one of which is ANSYS.

Programs which perform finite element analysis function in a similar way. To solve difficult problems, often where different physical phenomena are occurring simultaneously, an FEA model approximates an answer by breaking the model down into thousands of parts (hence the term "finite element"). Each of these "parts" or points is subject to the equations which govern the

situation, and with enough points and the correct boundary conditions, an accurate solution may be reached.

Finite element analysis, then, is a process which examines a discretized model of a continuous, real-world situation. Thus, not only the test sample, but also the equations governing the physics of the situation must be discretized. Obviously a series of discrete points cannot be described by systems of continuous equations. Instead these equations must be expressed in a format that enables them to interact with a discrete structural model.

What equations, then are involved in finite element analysis for a solid/fluid interface involving pressure waves? One needs to consider two equations simultaneously to evaluate the physics at the interface between a solid (specifically the Sound Cell block) and the fluid (through which the acoustic waves travel) (ANSYS Manual, Ch. 8).

The first equation is no surprise, it is the wave equation:

$$\frac{1}{c^2}\frac{\partial^2 P}{\partial t^2} - \nabla^2 P = 0 \qquad (19)$$

$$\nabla^2 = \frac{\partial^2}{\partial x^2} + \frac{\partial^2}{\partial y^2} + \frac{\partial^2}{\partial z^2} \qquad (20)$$

One will notice that the first differential term in equation (19) is "continuous" in that the time variable, *t* is not discrete. This equation, then is modified and takes the following form:

$$\frac{1}{c^2}\frac{\partial^2 P}{\delta t^2} - \nabla^2 P = 0 \qquad (21)$$

where c^2 is the speed of sound

In equation (21), the continuous pressure-time derivative has been modified. The δ denotes that the pressure is changing with respect to discrete units of time. The wave equation may be derived from equations of fluid physics, and a derivation (which includes important assumptions about the nature of sound waves) is given in *Appendix 4* on page 23.

The second equation which must be considered for analyzing a surface/fluid interface pertains to the nature of the surface itself. This equation is that of an accelerating mass that is subject to damping and a resilient spring (or "stiffness") force. The continuous form of this equation is as follows:

$$m\frac{d^2x}{dt^2} + b\frac{dx}{dt} + kx = F \qquad (22)$$

The first term in equation (22) is simply the mass multiplied by its acceleration. The second term, known as the "damping" term, is a function the velocity of the moving mass, and the final term (*kx*) is the "spring" term which is influenced by the displacement of the mass. Equation (22) is a "forced" or "driven" equation in that the right-hand side is non-zero. The mass is not simply moving after an initial displacement, but rather it is being "driven" by an external force.

This equation must also be discretized for use in finite element analysis. The form of the discretized equation is similar, but the continuous variables have been replaced by matrices. Equation (23) is the discretized form of equation (22).

$$[M]\{u''\} + [B]\{u'\} + [K]\{u\} = \{F^a\} \qquad (23)$$

where the matrices are defined as follows:

[M]	mass matrix
[B]	damping matrix
[K]	stiffness matrix
{u''}	acceleration vector
{u'}	velocity vector
{u}	displacement vector
$\{F^a\}$	applied load vector

Each of the matrices included in equation (23) pertains to the movement of a node on the surface. Each node is represented by an element in the mass matrix. This node is subject to a component of the applied load vector and therefore experiences a displacement, velocity, and acceleration, each of which is a specific component (unique to that node) in the corresponding matrices above.

FEA Input: Solid model to surface mesh

Several computer programs are capable of performing finite element analysis. A necessity for performing FEA is

the creation of a model which is composed of discrete points, as opposed to a continuous, solid mass. The creation of said points was not difficult. In fact, the interface between AutoCAD and CATT-Acoustic provided an easy way to obtain data about the discretization of the Sound Cell Block.

When a solid model is exported from AutoCAD to CATT, a geometry file is created that documents the vertices on each plane. This geometry file is simply a text file. Thus, one could create a mesh of small planes on the surface of the Sound Cell block in AutoCAD, and when exported, these planes would be defined by the vertices contained within the geometry file. It is these vertices that can function as the nodes for the finite element model.

Having the plane vertices in a text file (each defined by an x, y, and z coordinate) also has advantages because one can calculate the normals to each point in a program such as MatLab. Three programs that were written for examining the normal vectors for each plane on the Sound cell block are included in *Appendix 5* on page 25.

Looking to the Future

It was intended that ANSYS be the software utilized to perform the FEA on the Sound Cell block. Problems pertaining to accessing the software, however, have postponed the completion of this portion of the thesis investigation.

The investigation will continue however, and will be deemed complete when finite element analysis (whether in ANSYS, Fortran, or another software program) has been performed on the Sound Cell block, and the resulting data has been analyzed.

Currently, a discretized model of the Sound Cell block exists, as well as the necessary MatLab programs to find normal vectors and define normal vector matrices that correspond to the surface matrices. Thus, the only obstacle that remains is to manipulate the discretized model in such a way that it will interface with the chosen finite element analysis software.

Appendix 1*

The total pressure at a measurement point in front of the surface is given by the following equation:

$$p(x,y,z) = p_i(x,y,z) + \iint \left[G(x,y,z \mid x_o,y_o,\eta)\frac{\partial}{\partial n_o} p(x_o,y_o,\eta) - p(x_o,y_o,\eta)\frac{\partial}{\partial n_o} G(x,y,z \mid x_o,y_o,\eta) \right] dx_o dy_o \quad (4)$$

In equation (4) the $p_i(x,y,z)$ term represents the incident-reflected wave (p_i is a combination of the incident and reflected wave). Since this investigation examines scattering, only the second term is important for the present analysis. It should also be noted that the $^{\partial}/_{\partial n}$ operator is defined as follows.

$$\frac{\partial}{\partial n_o} = -\frac{\partial}{\partial z_o} + \frac{\partial \eta}{\partial x_o}\frac{\partial}{\partial x_o} + \frac{\partial \eta}{\partial y_o}\frac{\partial}{\partial y_o} \qquad (\text{if } \text{grad}_0\, \eta << 1) \quad (5)$$

If one assumes that the point of measurement for scattering at the coordinates (r, θ, φ) is far from area A, then the following approximation can be made for Green's function, which is included in the integrand of equation (4).

$$G \simeq \frac{e^{ikr}}{4\pi r}\left[e^{-ikz_o\cos\theta} + \frac{\cos\theta - \beta_0}{\cos\theta + \beta_0} e^{ikz_o\cos\theta} \right] e^{-ik\sin\theta(x_o\cos\varphi + y_o\sin\varphi)} \quad (6)$$

If the displacement from the xy plane ($\eta(x, y)$) is everywhere less than the wavelength of the incident sound, then the use of the Born approximation is valid. Mathematically, the Born approximation is a linearization of the exponential $e^x \approx x + 1$. The use of the Born approximation allows one to make the following substitutions inside the integral given in equation (4).

$$p \simeq P_i \frac{2\cos\theta_i}{\cos\theta_i + \beta}(1 - ik\beta z_o) e^{ik\sin\theta_i(x_o\cos\varphi_i + y_o\sin\varphi_i)} \quad (7)$$

$$G \simeq \frac{e^{ikr}}{4\pi r}\frac{2\cos\theta}{\cos\theta + \beta_o}(1 - ik\beta_o z_o) e^{-ik\sin\theta(x_o\cos\varphi + y_o\sin\varphi)} \quad (8)$$

One must now reevaluate the equation for the total pressure in front of the surface in question (situated in the xy plane). The equation for the total pressure not only takes into account the incident and reflected pressure, but the scattered pressure as well. The scattered portion of the total pressure is given in equation (9).

$$p_{scattered}(r) = P_i \frac{e^{ikr}}{r}\Phi(\theta,\varphi) \quad (9)$$

where

$$\Phi(\theta,\varphi) \simeq \frac{i}{\pi}\frac{\cos\theta_i\cos\theta}{(\cos\theta_i + \beta)(\cos\theta + \beta_0)} \iint [k(\beta - \beta_0) + \mu_x\frac{\partial\eta}{\partial x_0} + \mu_y\frac{\partial\eta}{\partial y_0}] e^{i(\mu_x x_0 + \mu_y y_0)} dx_0 dy_0 \quad (10)$$

In this case, the first term in the integrand goes to 0, since one initially assumed that the surface material has the same admittance (β_0) over then entire area. The vectors μ_x and μ_y are defined in equations (11) and (12), where k is simply the wave number defined as $2\pi/\lambda$.

$$\mu_x = k(\sin\theta_i\cos\varphi_i - \sin\theta\cos\varphi) \quad (11)$$

$$\mu_y = k(\sin\theta_i\sin\varphi_i - \sin\theta\sin\varphi) \quad (12)$$

To avoid any confusion as to what angles are being measured in the given equations, Figure 7 illustrates their spatial relationship.

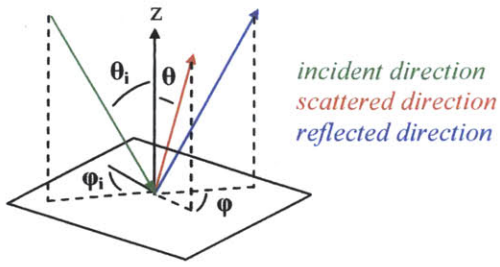

Figure 7

Equation (10) can be simplified if one chooses a fairly simple geometry to characterize the variation in the *z* coordinate over area *A* (i.e. choosing a straightforward form of $\eta(x, y)$). If one assumes that the "irregularity" over a given area is simply a raised rectangular region of height *h*, length ℓ, and width *w*, then the $(\partial\eta/\partial x_0)$ and $(\partial\eta/\partial y_0)$ terms simplify to the following.

$$\frac{\partial \eta}{\partial x_o} \simeq h[\delta(x_o + l/2) - \delta(x_o - l/2)] \qquad \text{for } -\tfrac{1}{2}w < y_0 < \tfrac{1}{2}w \tag{13}$$

$$\frac{\partial \eta}{\partial y_o} \simeq h[\delta(y_o + w/2) - \delta(y_o - w/2)] \qquad \text{for } -\tfrac{1}{2}\ell < x_0 < \tfrac{1}{2}\ell \tag{14}$$

Given these conditions, one can compute the integral given in equation (10). This integral equation is the angle distribution of the scattered wave. As shown in equation (9) this angle distribution acts to modify the magnitude of the scattered pressure. Should $\Phi(\theta,\varphi)$ be sufficiently small, one may ignore contribution of the scattered pressure to the total pressure propagating from the surface of the plane. Given the conditions imposed by equations (13) and (14), equation (10) may be reduced to the following expression.

$$\Phi(\theta_i, \varphi_i \mid \theta, \varphi) \simeq \frac{ikwkh\cos\theta_i \cos\theta}{\pi(\cos\theta_i + \beta_0)(\cos\theta + \beta_0)} \left[\gamma^2 \frac{\sin(\mu_x l/2)}{(\mu_x l/2)} \frac{\sin(\mu_y w/2)}{(\mu_y w/2)} \right] \tag{15}$$

where

$$\gamma^2 = \sin^2\theta_i + \sin^2\theta - 2\sin\theta_i \sin\theta \cos(\varphi_i - \varphi) \tag{16}$$

*** This derivation follows the derivation of the same equation given in Morse, 441-446 .**

Receiver	Distance from source in ft (for given angle of ascension)																	
	0	*5*	*10*	*15*	*20*	*25*	*30*	*35*	*40*	*45*	*50*	*55*	*60*	*65*	*70*	*75*	*80*	*85*
1	55.9																	
2	53.86	53.87	53.89	53.93	53.98	54.05	54.14	54.23	54.34	54.46	54.59	54.74	54.89	55.05	55.21	55.38	55.55	55.72
3	51.76	51.77	51.82	51.9	52.01	52.16	52.33	52.53	52.75	53	53.27	53.56	53.86	54.18	54.51	54.85	55.2	55.55
4	49.6	49.62	49.7	49.82	49.99	50.22	50.48	50.79	51.14	51.52	51.93	52.37	52.83	53.32	53.82	54.33	54.85	55.37
5	47.4	47.43	47.54	47.71	47.95	48.25	48.61	49.04	49.51	50.03	50.59	51.19	51.81	52.46	53.14	53.82	54.51	55.2
6	45.17	45.21	45.35	45.57	45.88	46.27	46.74	47.28	47.89	48.55	49.26	50.02	50.8	51.63	52.46	53.32	54.17	55.03
7	42.92	42.98	43.15	43.43	43.81	44.3	44.87	45.54	46.28	47.08	47.95	48.86	49.82	50.81	51.81	52.83	53.85	54.88
8	40.69	40.76	40.96	41.29	41.76	42.33	43.03	43.82	44.7	45.65	46.68	47.75	48.87	50.02	51.19	52.36	53.55	54.72
9	38.47	38.55	38.79	39.19	39.73	40.41	41.23	42.15	43.17	44.27	45.45	46.68	47.96	49.27	50.59	51.93	53.26	54.58
10	36.3	36.4	36.67	37.13	37.76	38.55	39.48	40.54	41.7	42.95	44.29	45.67	47.1	48.57	50.04	51.52	52.99	54.45
11	34.21	34.32	34.64	35.16	35.88	36.77	37.82	39.02	40.32	41.72	43.2	44.73	46.31	47.92	49.53	51.15	52.75	54.33
12	32.23	32.34	32.71	33.3	34.1	35.11	36.28	37.6	39.05	40.58	42.2	43.88	45.59	47.33	49.07	50.81	52.53	54.22
13	30.39	30.52	30.93	31.58	32.48	33.59	34.88	36.33	37.9	39.57	41.32	43.12	44.96	46.81	48.67	50.52	52.34	54.13
14	28.74	28.89	29.33	30.06	31.04	32.25	33.65	35.21	36.9	38.69	40.55	42.46	44.41	46.37	48.32	50.26	52.17	54.05
15	27.33	27.49	27.98	28.77	29.82	31.12	32.62	34.28	36.07	37.96	39.92	41.93	43.96	46.01	48.04	50.06	52.04	53.98
16	26.22	26.4	26.91	27.74	28.86	30.24	31.81	33.56	35.43	37.4	39.44	41.52	43.62	45.73	47.83	49.9	51.94	53.93
17	25.45	25.63	26.16	27.04	28.21	29.63	31.27	33.06	34.99	37.02	39.11	41.24	43.39	45.55	47.68	49.8	51.88	53.9
18	25.05	25.23	25.78	26.68	27.87	29.32	30.98	32.81	34.77	36.82	38.94	41.1	43.28	45.45	47.61	49.74	51.84	53.88
19	25.05	25.23	25.78	26.68	27.87	29.32	30.98	32.81	34.77	36.82	38.94	41.1	43.28	45.45	47.61	49.74	51.84	53.88
20	25.45	25.63	26.16	27.04	28.21	29.63	31.27	33.06	34.99	37.02	39.11	41.24	43.39	45.55	47.68	49.8	51.88	53.9
21	26.22	26.4	26.91	27.74	28.86	30.24	31.81	33.56	35.43	37.4	39.44	41.52	43.62	45.73	47.83	49.9	51.94	53.93
22	27.33	27.49	27.98	28.77	29.82	31.12	32.62	34.28	36.07	37.96	39.92	41.93	43.96	46.01	48.04	50.06	52.04	53.98
23	28.74	28.89	29.33	30.06	31.04	32.25	33.65	35.21	36.9	38.69	40.55	42.46	44.41	46.37	48.32	50.26	52.17	54.05
24	30.39	30.52	30.93	31.58	32.48	33.59	34.88	36.33	37.9	39.57	41.32	43.12	44.96	46.81	48.67	50.52	52.34	54.13
25	32.23	32.34	32.71	33.3	34.1	35.11	36.28	37.6	39.05	40.58	42.2	43.88	45.59	47.33	49.07	50.81	52.53	54.22
26	34.21	34.32	34.64	35.16	35.88	36.77	37.82	39.02	40.32	41.72	43.2	44.73	46.31	47.92	49.53	51.15	52.75	54.33
27	36.3	36.4	36.67	37.13	37.76	38.55	39.48	40.54	41.7	42.95	44.29	45.67	47.1	48.57	50.04	51.52	52.99	54.45
28	38.47	38.55	38.79	39.19	39.73	40.41	41.23	42.15	43.17	44.27	45.45	46.68	47.96	49.27	50.59	51.93	53.26	54.58
29	40.69	40.76	40.96	41.29	41.76	42.33	43.03	43.82	44.7	45.65	46.68	47.75	48.87	50.02	51.19	52.36	53.55	54.72
30	42.92	42.98	43.15	43.43	43.81	44.3	44.87	45.54	46.28	47.08	47.95	48.86	49.82	50.81	51.81	52.83	53.85	54.88
31	45.17	45.21	45.35	45.57	45.88	46.27	46.74	47.28	47.89	48.55	49.26	50.02	50.8	51.63	52.46	53.32	54.17	55.03
32	47.4	47.43	47.54	47.71	47.95	48.25	48.61	49.04	49.51	50.03	50.59	51.19	51.81	52.46	53.14	53.82	54.51	55.2
33	49.6	49.62	49.7	49.82	49.99	50.22	50.48	50.79	51.14	51.52	51.93	52.37	52.83	53.32	53.82	54.33	54.85	55.37
34	51.76	51.77	51.82	51.9	52.01	52.16	52.33	52.53	52.75	53	53.27	53.56	53.86	54.18	54.51	54.85	55.2	55.55
35	53.86	53.87	53.89	53.93	53.98	54.05	54.14	54.23	54.34	54.46	54.59	54.74	54.89	55.05	55.21	55.38	55.55	55.72
36	55.9																	

SPL for given receiver locations (90 dB source)

Receiver	0	5	10	15	20	25	30	35	40	45	50	55	60	65	70	75	80	85
1	65.4																	
2	65.7	65.7	65.7	65.7	65.7	65.7	65.6	65.6	65.6	65.6	65.6	65.6	65.5	65.5	65.5	65.5	65.4	65.4
3	66.0	66.0	66.0	66.0	66.0	66.0	65.9	65.9	65.9	65.8	65.8	65.7	65.7	65.6	65.6	65.5	65.5	65.4
4	66.4	66.4	66.4	66.4	66.3	66.3	66.3	66.2	66.1	66.1	66.0	65.9	65.9	65.8	65.7	65.6	65.5	65.5
5	66.8	66.8	66.8	66.7	66.7	66.6	66.6	66.5	66.4	66.3	66.2	66.1	66.0	65.9	65.8	65.7	65.6	65.5
6	67.2	67.2	67.2	67.1	67.1	67.0	66.9	66.8	66.7	66.6	66.5	66.3	66.2	66.1	65.9	65.8	65.6	65.5
7	67.7	67.7	67.6	67.6	67.5	67.4	67.3	67.1	67.0	66.9	66.7	66.5	66.4	66.2	66.0	65.9	65.7	65.5
8	68.1	68.1	68.1	68.0	67.9	67.8	67.6	67.5	67.3	67.1	66.9	66.7	66.5	66.3	66.1	65.9	65.7	65.6
9	68.6	68.6	68.5	68.5	68.3	68.2	68.0	67.8	67.6	67.4	67.2	66.9	66.7	66.5	66.2	66.0	65.8	65.6
10	69.1	69.1	69.0	68.9	68.8	68.6	68.4	68.2	67.9	67.7	67.4	67.1	66.9	66.6	66.3	66.1	65.8	65.6
11	69.6	69.6	69.5	69.4	69.2	69.0	68.8	68.5	68.2	67.9	67.6	67.3	67.0	66.7	66.4	66.1	65.9	65.6
12	70.2	70.1	70.0	69.9	69.7	69.4	69.1	68.8	68.5	68.2	67.8	67.5	67.1	66.8	66.5	66.2	65.9	65.6
13	70.7	70.6	70.5	70.3	70.1	69.8	69.5	69.1	68.7	68.4	68.0	67.6	67.3	66.9	66.6	66.2	65.9	65.6
14	71.1	71.1	71.0	70.8	70.5	70.1	69.8	69.4	69.0	68.6	68.2	67.8	67.4	67.0	66.6	66.3	66.0	65.7
15	71.6	71.5	71.4	71.1	70.8	70.5	70.0	69.6	69.2	68.7	68.3	67.9	67.5	67.1	66.7	66.3	66.0	65.7
16	71.9	71.9	71.7	71.5	71.1	70.7	70.3	69.8	69.3	68.9	68.4	68.0	67.5	67.1	66.7	66.4	66.0	65.7
17	72.2	72.1	72.0	71.7	71.3	70.9	70.4	69.9	69.4	68.9	68.5	68.0	67.6	67.1	66.8	66.4	66.0	65.7
18	72.3	72.3	72.1	71.8	71.4	71.0	70.5	70.0	69.5	69.0	68.5	68.0	67.6	67.2	66.8	66.4	66.0	65.7
19	72.3	72.3	72.1	71.8	71.4	71.0	70.5	70.0	69.5	69.0	68.5	68.0	67.6	67.2	66.8	66.4	66.0	65.7
20	72.2	72.1	72.0	71.7	71.3	70.9	70.4	69.9	69.4	68.9	68.5	68.0	67.6	67.1	66.8	66.4	66.0	65.7
21	71.9	71.9	71.7	71.5	71.1	70.7	70.3	69.8	69.3	68.9	68.4	68.0	67.5	67.1	66.7	66.4	66.0	65.7
22	71.6	71.5	71.4	71.1	70.8	70.5	70.0	69.6	69.2	68.7	68.3	67.9	67.5	67.1	66.7	66.3	66.0	65.7
23	71.1	71.1	71.0	70.8	70.5	70.1	69.8	69.4	69.0	68.6	68.2	67.8	67.4	67.0	66.6	66.3	66.0	65.7
24	70.7	70.6	70.5	70.3	70.1	69.8	69.5	69.1	68.7	68.4	68.0	67.6	67.3	66.9	66.6	66.2	65.9	65.6
25	70.2	70.1	70.0	69.9	69.7	69.4	69.1	68.8	68.5	68.2	67.8	67.5	67.1	66.8	66.5	66.2	65.9	65.6
26	69.6	69.6	69.5	69.4	69.2	69.0	68.8	68.5	68.2	67.9	67.6	67.3	67.0	66.7	66.4	66.1	65.9	65.6
27	69.1	69.1	69.0	68.9	68.8	68.6	68.4	68.2	67.9	67.7	67.4	67.1	66.9	66.6	66.3	66.1	65.8	65.6
28	68.6	68.6	68.5	68.5	68.3	68.2	68.0	67.8	67.6	67.4	67.2	66.9	66.7	66.5	66.2	66.0	65.8	65.6
29	68.1	68.1	68.1	68.0	67.9	67.8	67.6	67.5	67.3	67.1	66.9	66.7	66.5	66.3	66.1	65.9	65.7	65.6
30	67.7	67.7	67.6	67.6	67.5	67.4	67.3	67.1	67.0	66.9	66.7	66.5	66.4	66.2	66.0	65.9	65.7	65.5
31	67.2	67.2	67.2	67.1	67.1	67.0	66.9	66.8	66.7	66.6	66.5	66.3	66.2	66.1	65.9	65.8	65.6	65.5
32	66.8	66.8	66.8	66.7	66.7	66.6	66.6	66.5	66.4	66.3	66.2	66.1	66.0	65.9	65.8	65.7	65.6	65.5
33	66.4	66.4	66.4	66.4	66.3	66.3	66.3	66.2	66.1	66.1	66.0	65.9	65.9	65.8	65.7	65.6	65.5	65.5
34	66.0	66.0	66.0	66.0	66.0	66.0	65.9	65.9	65.9	65.8	65.8	65.7	65.7	65.6	65.6	65.5	65.5	65.4
35	65.7	65.7	65.7	65.7	65.7	65.7	65.6	65.6	65.6	65.6	65.6	65.6	65.5	65.5	65.5	65.5	65.4	65.4
36	65.4																	

CATT SPL by octave band								Difference in SPL levels					
Receiver	*125*	*250*	*500*	*1000*	*2000*	*4000*		*125*	*250*	*500*	*1000*	*2000*	*4000*
1	65.4	65.4	65.4	65.3	65.2	64.9		0.0	0.0	0.0	-0.1	-0.2	-0.5
2	65.7	65.7	65.7	65.7	65.6	65.2		0.0	0.0	0.0	0.0	-0.1	-0.5
3	66.1	66.1	66	66	65.9	65.6		0.1	0.1	0.0	0.0	-0.1	-0.4
4	66.4	66.4	66.4	66.4	66.3	66		0.0	0.0	0.0	0.0	-0.1	-0.4
5	66.8	66.8	66.8	66.8	66.7	66.4		0.0	0.0	0.0	0.0	-0.1	-0.4
6	67.2	67.2	67.2	67.2	67.1	66.8		0.0	0.0	0.0	0.0	-0.1	-0.4
7	67.7	67.7	67.7	67.6	67.6	67.3		0.0	0.0	0.0	-0.1	-0.1	-0.4
8	68.1	68.1	68.1	68.1	68	67.8		0.0	0.0	0.0	0.0	-0.1	-0.3
9	68.6	68.6	68.6	68.6	68.5	68.3		0.0	0.0	0.0	0.0	-0.1	-0.3
10	69.1	69.1	69.1	69.1	69	68.8		0.0	0.0	0.0	0.0	-0.1	-0.3
11	69.6	69.6	69.6	69.6	69.5	69.3		0.0	0.0	0.0	0.0	-0.1	-0.3
12	70.2	70.2	70.1	70.1	70.1	69.9		0.0	0.0	-0.1	-0.1	-0.1	-0.3
13	70.7	70.7	70.6	70.6	70.6	70.4		0.0	0.0	-0.1	-0.1	-0.1	-0.3
14	71.2	71.1	71.1	71.1	71.1	70.9		0.1	0.0	0.0	0.0	0.0	-0.2
15	71.6	71.6	71.6	71.6	71.5	71.3		0.0	0.0	0.0	0.0	-0.1	-0.3
16	71.9	71.9	71.9	71.9	71.9	71.7		0.0	0.0	0.0	0.0	0.0	-0.2
17	72.2	72.2	72.2	72.2	72.1	72		0.0	0.0	0.0	0.0	-0.1	-0.2
18	72.7	72.7	72.7	72.7	72.6	72.5		0.4	0.4	0.4	0.4	0.3	0.2
19	72.7	72.7	72.7	72.7	72.6	72.5		0.4	0.4	0.4	0.4	0.3	0.2
20	72.2	72.2	72.2	72.2	72.1	72		0.0	0.0	0.0	0.0	-0.1	-0.2
21	71.9	71.9	71.9	71.9	71.9	71.7		0.0	0.0	0.0	0.0	0.0	-0.2
22	71.6	71.6	71.6	71.6	71.5	71.3		0.0	0.0	0.0	0.0	-0.1	-0.3
23	71.2	71.1	71.1	71.1	71.1	70.9		0.1	0.0	0.0	0.0	0.0	-0.2
24	70.7	70.7	70.6	70.6	70.6	70.4		0.0	0.0	-0.1	-0.1	-0.1	-0.3
25	70.2	70.2	70.1	70.1	70.1	69.9		0.0	0.0	-0.1	-0.1	-0.1	-0.3
26	69.6	69.6	69.6	69.6	69.5	69.3		0.0	0.0	0.0	0.0	-0.1	-0.3
27	69.1	69.1	69.1	69.1	69	68.8		0.0	0.0	0.0	0.0	-0.1	-0.3
28	68.6	68.6	68.6	68.6	68.5	68.3		0.0	0.0	0.0	0.0	-0.1	-0.3
29	68.1	68.1	68.1	68.1	68	67.8		0.0	0.0	0.0	0.0	-0.1	-0.3
30	67.7	67.7	67.7	67.6	67.6	67.3		0.0	0.0	0.0	-0.1	-0.1	-0.4
31	67.2	67.2	67.2	67.2	67.1	66.8		0.0	0.0	0.0	0.0	-0.1	-0.4
32	66.8	66.8	66.8	66.8	66.7	66.4		0.0	0.0	0.0	0.0	-0.1	-0.4
33	66.4	66.4	66.4	66.4	66.3	66		0.0	0.0	0.0	0.0	-0.1	-0.4
34	66.1	66.1	66	66	65.9	65.6		0.1	0.1	0.0	0.0	-0.1	-0.4
35	65.7	65.7	65.7	65.7	65.6	65.2		0.0	0.0	0.0	0.0	-0.1	-0.5
36	65.4	65.4	65.4	65.3	65.2	64.9		0.0	0.0	0.0	-0.1	-0.2	-0.5

Appendix 4*

Starting with two simple equations in fluid physics, one can derive the wave equation (in this case without viscous dissipation). Two standard equations in fluid physics are the equation of continuity and Euler's equation. They are simply statements of the conservation of mass and the conservation of momentum, respectively. The equation of continuity is given as equation (24) and Euler's equation is given as equation (25).

$$\frac{\partial \rho}{\partial t} + \operatorname{div}(\rho \mathbf{v}) = 0 \tag{24}$$

$$\frac{\partial \mathbf{v}}{\partial t} + (\mathbf{v} \bullet \operatorname{grad})\mathbf{v} = -\frac{1}{\rho} \operatorname{grad} \mathrm{P} \tag{25}$$

In the above equations, ρ denotes the density, $\mathbf{v}$ the velocity, and P the pressure.

When considering an acoustical wave (i.e. a propagating pressure disturbance) one must first define the variables. The total pressure of the system is defined as $\mathrm{P} = \mathrm{P}_0 + \mathrm{P}'$ and the total density as $\rho = \rho_0 + \rho'$. The prime indicates the perturbed pressure and density. Two assumptions are made about the nature of ρ' and P'. They are as follows:

$\rho' << \rho_0$

$\mathrm{P}' << \mathrm{P}_0$

After substituting $\rho = \rho_0 + \rho'$ into equation (24) one obtains the following form of the continuity equation (the vector form of the equation is given as well).

$$\frac{\partial \rho'}{\partial t} + \rho_0 \operatorname{div} \mathbf{v} = 0 \tag{26}$$

$$\frac{\partial \rho'}{\partial t} + \rho_0 \nabla \bullet \mathbf{v} = 0$$

Substituting both $\mathrm{P} = \mathrm{P}_0 + \mathrm{P}'$ and $\rho = \rho_0 + \rho'$ into Euler's equation (equation 25) and taking note of the assumptions regarding ρ' and P' yields the following result.

$$\frac{\partial \mathbf{v}}{\partial t} + (\mathbf{v} \bullet \operatorname{grad})\mathbf{v} = -\frac{1}{\rho_0} \operatorname{grad} \mathrm{P}' \tag{27}$$

$$\frac{\partial \mathbf{v}}{\partial t} + (\mathbf{v} \bullet \nabla)\mathbf{v} = -\frac{1}{\rho_0} \nabla \mathrm{P}'$$

Because the oscillations of the fluid particles are small, the velocity of the particles is small as well, so one may neglect the grad term on the left side of the equation. Thus, equation (27) reduces to

$$\frac{\partial \mathbf{v}}{\partial t} = -\frac{1}{\rho_0} \nabla \mathrm{P}' \tag{28}$$

If one assumes that the fluid in question is ideal, and that the changes within the fluid brought about by the perturbations are adiabatic, then the following relationship is true:

$$P' = \left(\frac{\partial P}{\partial \rho_0}\right)_s \rho' \tag{29}$$

$$\rho' = \frac{1}{\left(\frac{\partial P}{\partial \rho_0}\right)_s} P'$$

Substituting equation (29) into the modified form of the continuity equation (equation (26)) yields the following:

$$\frac{\partial P'}{\partial t} + \rho_0 \left(\frac{\partial P}{\partial \rho_0}\right)_s \operatorname{div} \mathbf{v} = 0 \tag{30}$$

At this point it is worth pausing to take a look at derived equations (28) and (30). Each equation has two unknowns, **v** and P'. It is useful to introduce the velocity potential **v** = grad Φ. In this way, all of the unknown variables may be expressed in terms of another variable, Φ. Integrating equation (28), one gains the equation (31).

$$\mathbf{v}(t) = -\frac{1}{\rho_0} P' \tag{31}$$

One can then substitute grad Φ for **v** in equation (31). Having made this substitution, and solving equation (31) for P' one has an expression that can be substituted into equation (30). Equation 30 then becomes

$$\frac{\partial}{\partial t}\left(-\rho_0 \frac{\partial \Phi}{\partial t}\right) + \rho_0 \left(\frac{\partial P}{\partial \rho_0}\right)_s \operatorname{div} \mathbf{v} = 0 \tag{32}$$

$$-\frac{\partial^2 \Phi}{\partial t^2} + \left(\frac{\partial P}{\partial \rho_0}\right)_s \operatorname{div} \mathbf{v} = 0$$

Remembering once again that **v** = grad Φ, and defining the sound speed squared (c^2) as derivative in front of the divergence term, equation (32) takes on the familiar form of the wave equation, given below.

$$\frac{\partial^2 \Phi}{\partial t^2} - c^2 \operatorname{div}(\nabla \Phi) = 0$$

$$\frac{\partial^2 \Phi}{\partial t^2} - c^2 \nabla^2 \Phi = 0$$

$$\frac{1}{c^2}\frac{\partial^2 \Phi}{\partial t^2} - \nabla^2 \Phi = 0 \tag{33}$$

***This derivation follows the derivation of the same equation given in Landau, 251-252.**

Appendix 5

These MatLab programs were designed to be run one after another. Prior to running the first program, one would import the text file containing the data points for a given plane. This text file then becomes a variable within MatLab, having the name 'S#' where # is a plane index number.

The first program was designed to give a basic scatter plot of a given matrix (describing one of the twenty planes that compose the block). Based on this plot one can discern which normal vector is oriented properly to the plane.

```
%Input the Surface for which the points are being plotted
Snumber=input('Indicate surface being evaluated ');

%Extracts 1st column vector from S_ matrix (contains x,y,z coordinates)
A=Snumber(:,1);

%Extracts 2nd column vector from S_ matrix
B=Snumber(:,2);

%Extracts 3rd column vector from S_ matrix
C=Snumber(:,3);

plot3(A,B,C,'.')
```

The second program was written to find the unit normal vector to a plane, given three points that are found on the plane. Since one can take the cross product of two vectors in two ways (the cross product is not commutative, $i \times j \neq j \times i$), this program finds both unit normal vectors, and a comparison with the scatter plot reveals the normal with the correct orientation.

```
%Input the Surface for which the normal is being found
Snumber=input('Indicate surface being evaluated ');

%Extracts 1st row vector from S_ matrix (contains x,y,z coordinates)
P=Snumber(1,:);

%Extracts 2nd row vector from S_ matrix
Q=Snumber(2,:);

%Extracts 3rd row vector from S_ matrix
R=Snumber(3,:);

%Cross product of vectors PQ and PR (the "non-unit" normal vector)
c1=cross((Q-P),(R-P));
c2=cross((R-P),(Q-P));

%Calculating unit normal
  %Extracts components of cross product 1
  c1x=c1(:,1);
  c1y=c1(:,2);
  c1z=c1(:,3);
  %Finds magnitude of first normal
  length1=norm(c1);

    %Unit vector components
    u1x=c1x/length1;
    u1y=c1y/length1;
```

```
    u1z=c1z/length1;

  %Extracts components of cross product 2
  c2x=c2(:,1);
  c2y=c2(:,2);
  c2z=c2(:,3);
  %Finds magnitude of second normal
  length2=norm(c2);

    %Unit vector components
    u2x=c2x/length2;
    u2y=c2y/length2;
    u2z=c2z/length2;

%Unit normal vectors
n1=[u1x,u1y,u1z]
n2=[u2x,u2y,u2z]
```

The third program creates a matrix containing unit normals for each point in the original surface matrix (denoted by S#).

```
%Input the Surface for which the normal matrix is being found
Snumber=input('Indicate surface being evaluated ');

%Finds the size of the Surface matrix in question
[m,n]=size(Snumber);

%Creates a blank matrix with same dimensions as Surface matrix
N=zeros(m,n);

%Input which normal vector is correct for surface in question
v=input('Input correct normal vector, 1 or 2 ');

%Defines new unit normal matrix based on correct normal direction
if (v == 1)
  N(:,1)=u1x;
  N(:,2)=u1y;
  N(:,3)=u1z;
end

if (v == 2)
  N(:,1)=u2x;
  N(:,2)=u2y;
  N(:,3)=u2z;
End
```

Works Cited

Cavanaugh, William J., and Joseph A. Wilkes. Architectural Acoustics. New York: John Wiley and Sons, Inc., 1999.

Cox, Trevor, et al. "AES information document for room acoustics and sound reinforcement systems – Characterization and measurement of surface scattering uniformity." Audio Engineering Society, 2001.

Cox, Trevor, and Peter D'Antonio. Acoustic Absorbers and Diffusers: Theory, Design and Application. New York: Spon Press, 2004.

Hecht, Eugene. Optics. 4th ed. Boston: Addison Wesley, 2002.

Landau, L.D., and E.M. Lifshitz. Fluid Mechanics. 2nd ed. Boston: Elsevier Butterworth-Heinemann, 2004.

Morse, Philip M., and K. Uno Ingard. Theoretical Acoustics. Princeton: Princeton University Press, 1968.